Dynamics of molten alkali halides: LiCl and DCl

1989 J. Phys.: Condens. Matter 1 2369

(http://iopscience.iop.org/0953-8984/1/13/010)

J. Phys.: Condens. Matter 1 (1989) 2369–2380. Printed in the UK

Dynamics of molten alkali halides: LiCl and KCl

L Pusztai† and R L McGreevy
Clarendon Laboratory, Parks Road, Oxford OX1 3PU, UK

Received 21 September 1988, in final form 7 November 1988

Abstract. We have measured the inelastic neutron scattering spectra of three samples of molten ^{7}LiCl with different isotopic chlorine compositions, and of one sample of molten KCl, using the time-of-flight spectrometer IN6 at the Institut Laue–Langevin. It is observed that the main peak in the total dynamical structure factor for LiCl is sharply peaked in both Q and ω directions, while that for KCl is much weaker and broader. The spectra for LiCl show evidence for two types of collective mode with characteristic energies of 10–20 and 40–50 meV. Using the differences between the samples, it is possible to show that appropriate pairs of dynamical variables for these modes are m_+, $-m_-$ (low energies) and q_+, $-q_-$ (high energies), whereas in molten CsCl the variables have been shown to be m_+, m_- and q_+, q_-. We propose that for the alkali chlorides (where the ionic radius ratio $r_+/r_- < 1$) the former variables are appropriate when $m_+ < m_-$, and the latter when $m_+ > m_-$. There is a crossover between the variables, resulting in strong-mode coupling, when $m_+ = m_-$. The data for KCl are consistent with this proposition.

1. Introduction

It is now well established that the technique of isotopic substitution may be used in inelastic neutron scattering experiments to separate the principal dynamic modes in liquids (see, e.g., McGreevy 1987). By a first-order difference a substantial separation of mass (acoustic mode) and charge (optic mode) currents has been achieved in the momentum transfer range $2\ \text{Å}^{-1} < Q < 4\ \text{Å}^{-1}$ in molten RbCl (McGreevy and Mitchell 1982) and CsCl (McGreevy *et al* 1985). In $SrCl_2$ a qualitative second-order difference has been used to show that the 'additional' modes observed are not related to mass or charge currents (Margaca *et al* 1984). More recently, quantitative second-order differences have been made in molten NiI_2 (Wood 1988).

From theory and computer simulation, we know that at low Q (less than $0.5\ \text{Å}^{-1}$) the mass and charge currents in molten alkali halides are largely independent (this being strictly true at $Q = 0$) and their power spectra peak at frequencies close to those of the acoustic and optic modes in the corresponding crystals. At higher Q (greater than $10\ \text{Å}^{-1}$), mass and charge currents are strongly coupled and the independent dynamical variables are ion type, this being the free-particle response limit. In the intermediate-Q range the dynamical behaviour will reflect the short-range structural order, and the choice of appropriate (i.e. substantially independent) dynamical variables is not obvious.

† Permanent address: Laboratory of Theoretical Chemistry, L Eotvos University, Muzeum krt 6–8, Budapest H-1088, Hungary.

0953-8984/89/132369 + 12 $02.50

In this paper, we report on inelastic neutron scattering studies of molten LiCl (with isotopic substitution) and KCl. The aim of the experiments is to determine whether mass and charge are good dynamical variables in the range $2\ \text{Å}^{-1} < Q < 4\ \text{Å}^{-1}$ for all alkali chlorides, or if the variables change as the local structure changes from octahedral coordination in CsCl (Locke *et al* 1985) to tetrahedral coordination in LiCl (Howe and McGreevy 1988).

2. Scattering cross sections

The dynamics of a multi-component system can be described in terms of the density or current fluctuations of either the properties or the types of particle in the system. The definitions of densities and currents and their correlation functions used here are those given by McGreevy *et al* (1984) and Margaca *et al* (1984).

The differential cross section for neutron scattering from a binary ionic melt can be written in terms of the self-dynamical structure factors $S^{\mathrm{s}}_{\alpha}(Q, \omega)$ and partial dynamical structure factors $S_{\alpha\beta}(Q, \omega)$ as

$$\begin{aligned}(1/N)[\mathrm{d}^2\sigma/(\mathrm{d}\Omega\,\mathrm{d}\omega)] &= (k/k_0)[(\overline{b_+^2} - \bar{b}_+^2)S^{\mathrm{s}}_+(Q,\omega) + (\overline{b_-^2} - \bar{b}_-^2)S^{\mathrm{s}}_-(Q,\omega) \\ &\quad + \bar{b}_+^2 S_{++}(Q,\omega) + \bar{b}_-^2 S_{--}(Q,\omega) + 2\bar{b}_+\bar{b}_- S_{+-}(Q,\omega)] \\ &= (k/k_0)\overline{b^2} S_{\mathrm{T}}(Q,\omega). \end{aligned} \tag{1}$$

N is the total number of ions, $\boldsymbol{k}_0$ and $\boldsymbol{k}$, respectively, are the incident and scattered neutron wavevectors, $\boldsymbol{Q} = \boldsymbol{k}_0 - \boldsymbol{k}$ is the momentum transfer and $\hbar\omega$ is the energy transfer. $\bar{b}_\alpha$ is the coherent scattering length and $4\pi\overline{b_\alpha^2}$ the total scattering cross section for atoms of type α. $4\pi\overline{b^2} = 2\pi(\overline{b_+^2} + \overline{b_-^2})$ is the average cross section per atom. $S_{\mathrm{T}}(Q, \omega)$ is the total (neutron-weighted) dynamical structure factor.

Alternatively the differential cross section may be written in terms of any two properties or dynamical variables (A, B) of the system, with the corresponding partial dynamical structure factors

$$\begin{aligned} S_{AB}(Q,\omega) &= [A_+B_+S_{++}(Q,\omega) + A_-B_-S_{--}(Q,\omega) \\ &\quad + (A_+B_- + A_-B_+)S_{+-}(Q,\omega)]/(|A_+| + |A_-|)(|B_+| + |B_-|) \end{aligned} \tag{2}$$

where A_α is the value of property or dynamical variable A for atoms of type α. Typical properties are number (N: $A_+ = 1, A_- = 1$), mass (m: $A_+ = m_+, A_- = m_-$) and charge (q: $A_+ = q_+, A_- = q_-$). The cross section then becomes

$$\begin{aligned}(1/N)[\mathrm{d}^2\sigma/(\mathrm{d}\Omega\,\mathrm{d}\omega)] &= (k/k_0)[(\overline{b_+^2} - \bar{b}_+^2)S^{\mathrm{s}}_+(Q,\omega) + (\overline{b_-^2} - \bar{b}_-^2)S^{\mathrm{s}}_-(Q,\omega) \\ &\quad + a_A^2 S_{AA}(Q,\omega) + a_B^2 S_{BB}(Q,\omega) + 2a_A a_B S_{AB}(Q,\omega)] \end{aligned} \tag{3}$$

where

$$a_A = (\bar{b}_+B'_- - \bar{b}_-B'_+)/(A'_+B'_- - A'_-B'_+) \tag{4}$$

$$a_B = (\bar{b}_+A'_- - \bar{b}_-A'_+)/(B'_+A'_- - B'_-A'_+) \tag{5}$$

and

$$A'_+ = A_+/(|A_+| + |A_-|) \qquad \text{etc.} \tag{6}$$

The cross section may also be written in terms of the power spectra of the longitudinal current correlations

Table 1. Sample compositions and scattering parameters.

	$^{7}Li^{37}Cl$	$^{7}LiCl$	$^{7}Li^{35}Cl$	KCl
Amount of ^{37}Cl (%)	95.0	24.47	0.37	24.47
Amount of ^{35}Cl (%)	5.0	75.53	99.63	75.53
$\overline{b_+^2}$ (10^{-24} cm^2)	0.115	0.115	0.115	0.167
$\overline{b_-^2}$ (10^{-24} cm^2)	0.176	1.323	1.714	1.323
$\bar{b}_+ = a_+$ (10^{-12} cm)	−0.220	−0.220	−0.220	0.367
$\bar{b}_- = a_-$ (10^{-12} cm)	0.351	0.959	1.167	0.959
$a_+^2/\overline{b^2}$	0.333	0.067	0.053	0.181
$a_-^2/\overline{b^2}$	0.897	1.279	1.489	1.234
$a_m^2/\overline{b^2}$	0.118	0.760	0.981	2.360
$a_q^2/\overline{b^2}$	1.608	0.648	0.624	0.578
$a_m^2/\overline{b^2}$	2.241	1.933	2.104	0.470
a_q^2/b^2	1.744	0.016	0.0	2.463

$$C_{AB}^{L}(Q, \omega) = \omega^2 S_{AB}(Q, \omega) \tag{7}$$

as

$$\begin{aligned}(1/N)[\mathrm{d}^2\sigma/(\mathrm{d}\Omega\,\mathrm{d}\omega)] &= (k/k_0)(1/\omega^2)[\omega^2(\overline{b_+^2} - \bar{b}_+^2)S_+^s(Q,\omega) + \omega^2(\overline{b_-^2} - \bar{b}_-^2)S_-^s(Q,\omega) \\ &\quad + a_A^2 C_{AA}^{L}(Q,\omega) + a_B^2 C_{BB}^{L}(Q,\omega) + 2a_A a_B C_{AB}^{L}(Q,\omega)] \\ &= (k/k_0)(\overline{b^2}/\omega^2)C_T^{L}(Q,\omega)\end{aligned} \tag{8}$$

where $C_T^{L}(Q, \omega)$ is the power spectrum of the total (neutron-weighted) longitudinal current.

3. Experimental details

Three samples of molten $^{7}LiCl$ with different isotropic chlorine compositions, and one of molten KCl, were studied by inelastic scattering of 5.1 Å neutrons using the IN6 time-of-flight spectrometer at the Institut Laue–Langevin, Grenoble. Details of sample compositions and scattering parameters are given in table 1. The ^{7}Li isotope was used because of the high neutron absorption cross-section of ^{6}Li. The anhydrous samples were contained under vacuum in sealed vanadium cylinders of approximate dimensions 5 × 1 cm. Spectra were measured for the samples (LiCl at 900 K, and KCl at 1050 K, for 12–18 h per sample), an empty sample container (900 K for 12 h) and the empty furnace (300 K for 3 h). The correction and normalisation of all sets of data followed the procedures described in detail by McGreevy *et al* (1984).

4. Results

Corrected and normalised intensities for molten $^{7}LiCl$ at six scattering angles are shown in figure 1. The spectra have the characteristic features of an ionic melt: a broad quasi-elastic peak (QEP) at a low energy, associated with diffusion, together with an extended inelastic spectrum at a higher energy, associated with collective modes. In this figure the intensity is plotted as a function of the time of flight τ at a fixed scattering angle θ. Both

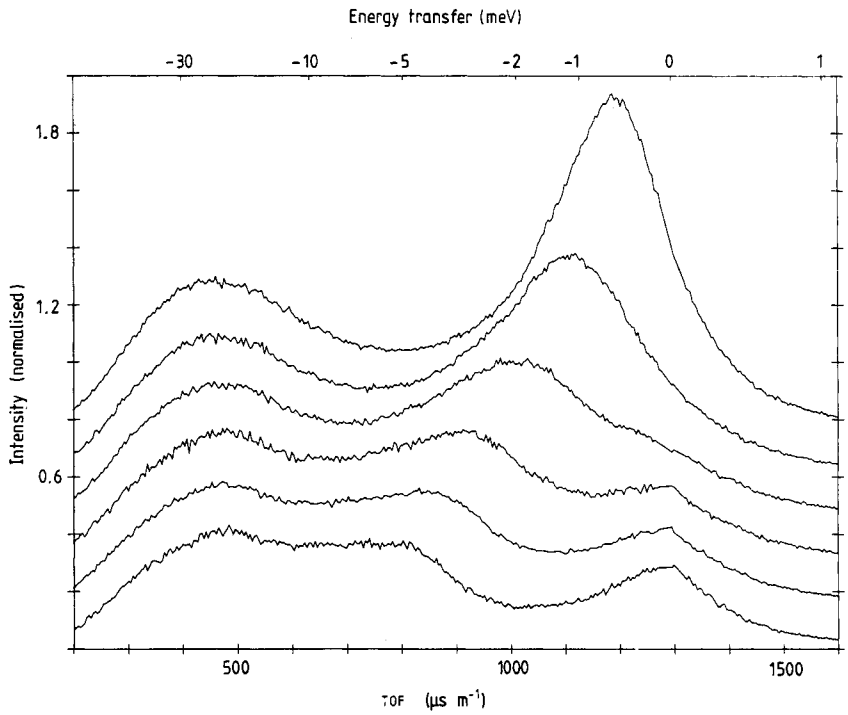

Figure 1. Corrected and normalised intensities for molten LiCl at a temperature of 900 K. The curves, in ascending order, are at scattering angles of 66.80, 72.70, 78.60, 84.60, 91.40 and 98.20. The vertical scale is shifted by 0.15 between curves. (TOF ≡ time of flight.)

Q and ω vary with τ, and the relation between intensity and dynamical structure factor is of the form

$$I(\theta, \tau) \propto (\omega_0 - \omega)^2 S_T(Q, \omega) \tag{9}$$

where $\hbar\omega_0 \simeq 3.5$ meV is the incident neutron energy. Around the QEP, $\omega \simeq 0$ and so $I \propto S_T(Q, \omega)$. For $\omega \gg \omega_0$, $I \propto \omega^2 S_T(Q, \omega) = C_T^L(Q, \omega)$ and hence the inelastic spectrum corresponds to the longitudinal current.

It should be noted that the QEP, centred at around $E = \hbar\omega = 0$, is weak at $\theta = 66.8°$ and apparently decreases in intensity and disappears as θ increases. A peak in the inelastic spectrum at $E \simeq 5$ meV at 66.8° decreases in energy and increases in intensity as θ increases, peaking at about 0.5 meV at 98.2°. The origin of this effect can be understood by examining $S_T(Q, \omega)$ (figure 2). This has been produced by interpolating the spectra onto a grid of constant Q, E points. At $E = 0$ the peak at $Q \simeq 2$ Å^{-1}, corresponding to the first peak in the static structure factor $S_T(Q)$, is exceptionally strong and narrow, and it can be seen that the tail of this peak extends out in energy so that there is still a peak at 2 Å^{-1} at $E = 7$ meV. $S_T(Q, \omega)$ has a similar form for the other two LiCl samples. In other alkali chlorides the tails normally extend less than 1 meV (see, e.g., McGreevy *et al* 1985). This tail runs at constant Q; so the experimental spectra, taken at a constant scattering angle, cut across it diagonally, producing the effect noted above. (The cut-offs in figure 2, indicated by the thick curves, correspond to the Q, ω loci of the lowest and highest scattering angles, and the loci of all other angles run approximately parallel to these.) Howe and McGreevy (1988) have proposed that

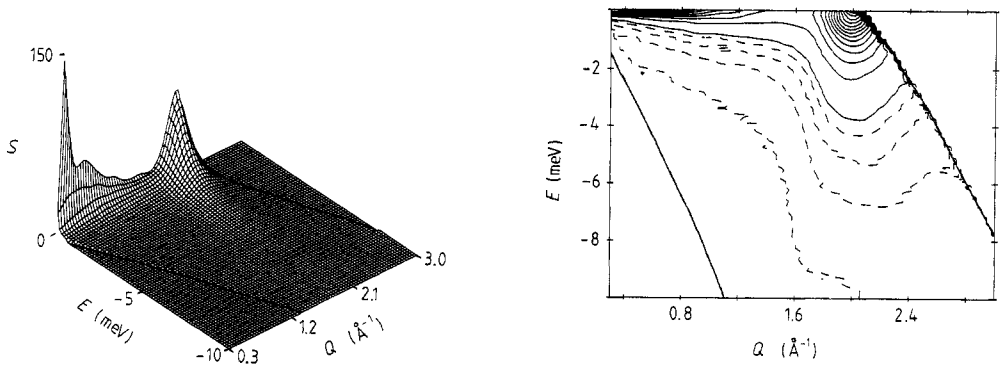

Figure 2. $S_T(Q, \omega)$ for molten LiCl: — — —, heights of 1, 2, 3 and 4; ———, heights of 5, 10, 15, 20, etc.

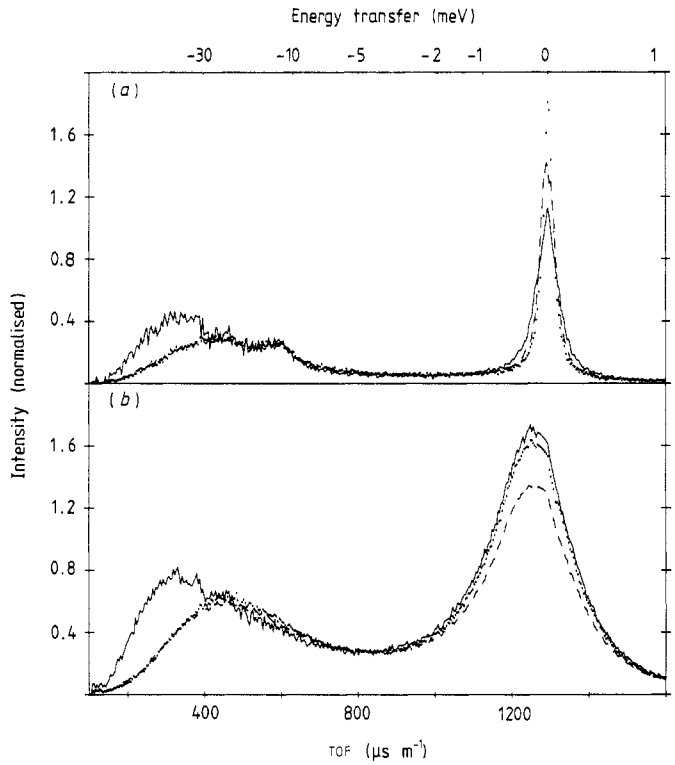

Figure 3. Corrected and normalised intensities for molten $Li^{37}Cl$ (———), LiCl (— — —) and $Li^{35}Cl$ (. . .) at scattering angles of (*a*) 21.3 and (*b*) 106.4.

inconsistencies around the first structure factor peak in their diffraction data for molten LiCl are due to poor inelasticity corrections caused by just such an effect. This is confirmed by the data shown here.

Figure 3 shows corrected and normalised intensities for all three LiCl samples at two scattering angles. In the region of energy transfer 1 meV $< E <$ 20 meV the spectra are almost identical (note from equations (1) and (9) that the intensities are normalised by

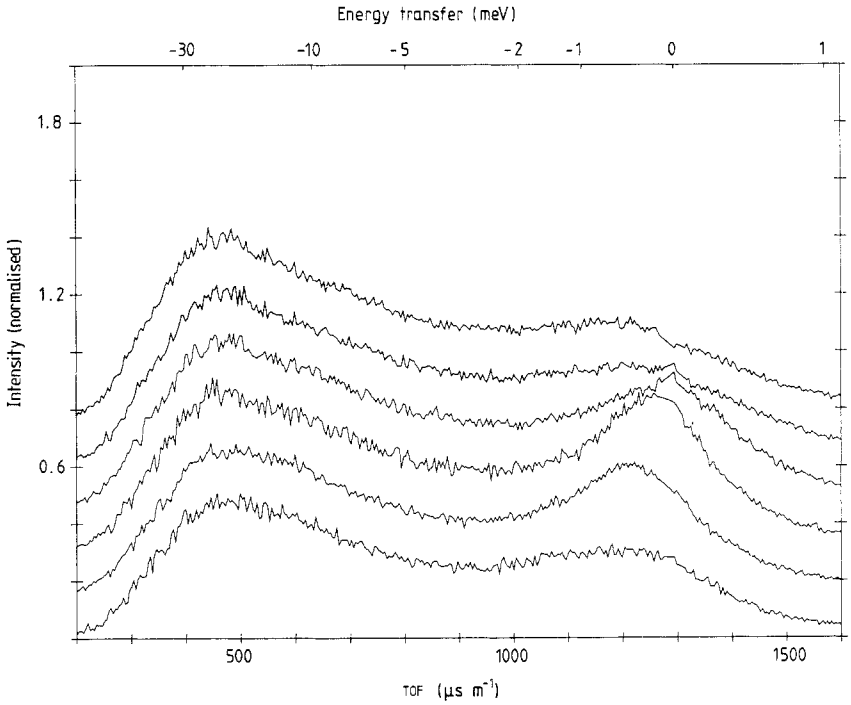

Figure 4. Corrected and normalised intensities for molten KCl at a temperature of 1050 K. The curves, in ascending order, are at scattering angles of 66.80, 72.70, 78.60, 84.60, 91.40 and 98.20. The vertical scale is shifted by 0.15 between curves.

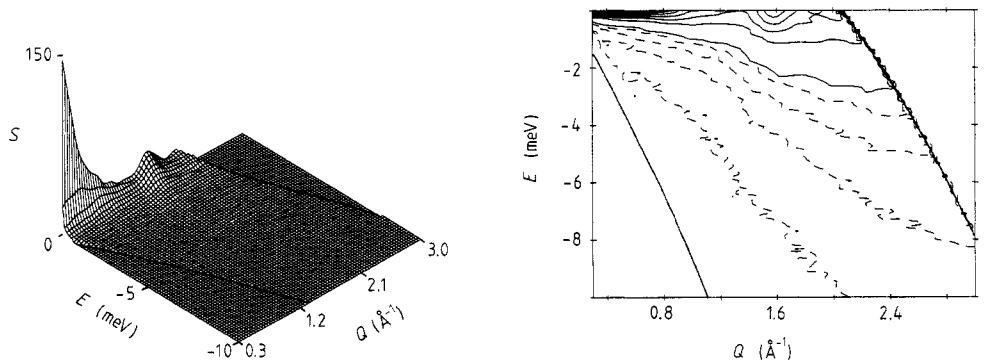

Figure 5. $S_T(Q, \omega)$ for molten KCl: — — —, heights of 1, 2, 3 and 4; ———, heights of 5, 10, 15, 20 etc.

the total scattering cross section for the particular sample). However, for $E > 20$ meV the $^7Li^{37}Cl$ spectrum is significantly higher, with a peak at $E = 40$–50 meV. This may be compared with CsCl (McGreevy *et al* 1985) where the $Cs^{37}Cl$ sample is lower at high energies.

In figure 4, we show corrected and normalised intensities for molten KCl. These are significantly different from those for LiCl around the QEP. $S_T(Q, \omega)$ is shown in figure 5. At $E = 0$ there is a small peak at $Q = 1.6$ Å^{-1} which extends in energy less than 1 meV.

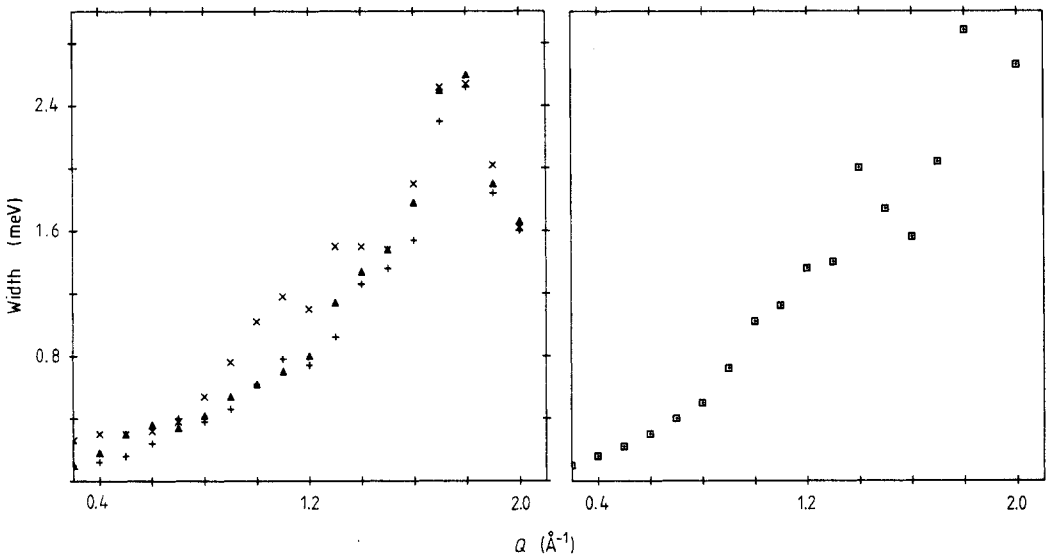

Figure 6. The full width at half height of $S_T(Q, \omega)$ for molten $Li^{37}Cl$ (△), LiCl (+), $Li^{35}Cl$ (×) and KCl (□).

There is an even weaker peak at 2 $Å^{-1}$, although for $E > 4$ meV at this Q-value $S_T(Q, \omega)$ is of equal intensity to that for LiCl. The static structure factor

$$S_T(Q) = \int S_T(Q, \omega)\, d\omega \tag{10}$$

in this Q region therefore contains a significantly larger contribution from high ω in KCl than in LiCl.

The full widths at half-height of $S_T(Q, \omega)$ are shown in figure 6. In the case of the LiCl samples there is a pronounced narrowing at around $Q = 2$ $Å^{-1}$, whereas in KCl there is a minimum at 1.6 $Å^{-1}$, both relating to the corresponding peaks in $S_T(Q)$. These may possibly be due to the phenomenon of de Gennes (1959) narrowing where the peak narrows as the height increases in order to maintain the correct second moment.

5. Choice of dynamical variables

In principle, we wish to describe the dynamics of molten alkali halides in terms of two independent dynamical variables, in the same way that there are two types of independent mode (acoustic and optic) along symmetry directions in the crystal (harmonic approximation). In order for the variables to be independent, the cross-correlation $S_{AB}(Q, \omega)$, or equivalently all the moments

$$\langle \omega^n S_{AB} \rangle = \int_{-\infty}^{\infty} \omega^n S_{AB}(Q, \omega)\, d\omega \tag{11}$$

should be zero. In practice, this is not possible for an N-particle system with only short-range structural order; so we simply require that for the variables to be useful the lower-order moments should be small. The zeroth moment $\langle S_{AB} \rangle$ is the partial structure factor

$S_{AB}(Q)$, while the second moment is the integral of the partial longitudinal current $C^{L}_{AB}(Q, \omega)$. Classically the odd moments are all zero (ignoring small recoil effects).

Since there are five contributions to the total dynamical structure factor (equation (1)), we require fifth-order isotopic substitution to make a complete separation of all the partial dynamical structure factors. This is totally impractical because isotopic differences are too small and experimental errors too large; in most cases, only first-order differences can be achieved. We therefore have to make certain assumptions when attempting to determine dynamical variables. Firstly, we assume that the self-dynamical terms S^{s}_{+} and S^{s}_{-} contribute significantly only in the quasi-elastic region ($E < 1$ meV) and that the inelastic scattering is dominated by the three partial currents C^{L}_{AA}, C^{L}_{BB} and C^{L}_{AB}. If the variables A and B are largely independent, then C^{L}_{AB} will be small and C^{L}_{AA} and C^{L}_{BB} will peak at well separated energies. If A and B are strongly coupled, then C^{L}_{AB} will be large and C^{L}_{AA} and C^{L}_{BB} will have either one or two peaks at the same energy or energies. A suitable choice of variables may be therefore made using only first-order differences.

It is apparent from the spectra shown in figure 3 that there is a peak at $E = 40$–50 meV for $^{7}Li^{37}Cl$ that is absent in the other two samples, while the peaks at 10–30 meV are of equal intensity in all three samples. If we presume that these peaks correspond to different collective modes, then we need to choose dynamical variables A and B to describe the system for which $a_B^2/\overline{b^2} \simeq 0$ for $^{7}LiCl$ and $^{7}Li^{35}Cl$ and $a_B^2/\overline{b^2} \neq 0$ for $^{7}Li^{37}Cl$, and the values of $a_A^2/\overline{b^2}$ are approximately equal for all three samples. It is apparent from the coefficients given in table 1 that neither mass and charge (a_m and a_q) nor ion type (a_+ and a_-) satisfy these criteria.

If we assume that $a_B = 0$ for $^{7}LiCl$ then, from equation (5), $A_-/A_+ = -4.359$. Assuming that $a_A^2/\overline{b^2}$ for $^{7}Li^{35}Cl$ is equal to that for $^{7}Li^{37}Cl$ gives, from equation (4), $B_-/B_+ = 0.869$. Since $-m_-/m_+ \simeq -5.07$ (depending on isotope) and $-q_-/q_+ = 1.0$, we suggest that appropriate variables may be m_+, $-m_-$ and q_+, $-q_-$, which we shall denote as $\bar{m}$ and $\bar{q}$. For an alkali halide $\bar{q} \equiv N$, although this would not be the case for an alkaline-earth halide where $|q_+| \neq |q_-|$. Coefficients $a_{\bar{m}}$ and $a_{\bar{q}}$ for the three LiCl samples are given in table 1, and it can be seen that they satisfy the above criteria.

Since the spectra for $^{7}LiCl$ and $^{7}Li^{35}Cl$ are so similar, it is not possible, given the statistical accuracy of the experiment, to take second-order differences to separate the relevant partial dynamical structure factors. We have therefore calculated the combinations

$$0.475S_T(^{7}Li^{35}Cl) = S_{\bar{m}\bar{m}} - 0.026S_{\bar{m}\bar{q}} + 0.035S^{s}_{+} + 0.183S^{s}_{-} = \hat{S}_{\bar{m}\bar{m}} \tag{12}$$

and

$$0.572S_T(^{7}Li^{37}Cl) - 0.609S_T(^{7}Li^{35}Cl) = S_{\bar{q}\bar{q}} + 2.123S_{\bar{m}\bar{q}} + 0.219S^{s}_{+} + 0.026S^{s}_{-} = \hat{S}_{\bar{q}\bar{q}}. \tag{13}$$

Corresponding scattering intensities ($\hat{I} \propto (\omega_0 - \omega)^2\hat{S}$) are shown in figure 7, from which it can be seen that in the inelastic region a good separation of the peaks has indeed been achieved, and $\bar{m}$ and $\bar{q}$ are therefore useful dynamical variables. A quasi-dispersion curve has been derived from the peak positions of $\hat{C}^{L}_{mm}(Q, \omega)$ and $\hat{C}^{L}_{qq}(Q, \omega)$ at constant Q (figure 8). There are two branches, widely separated in energy over the whole experimental range. However, it should be noted that the $\bar{q}$ branch, because of its high energy, corresponds to a different Q-range from the $\bar{m}$ branch. The separation may be smaller at equal Q-values.

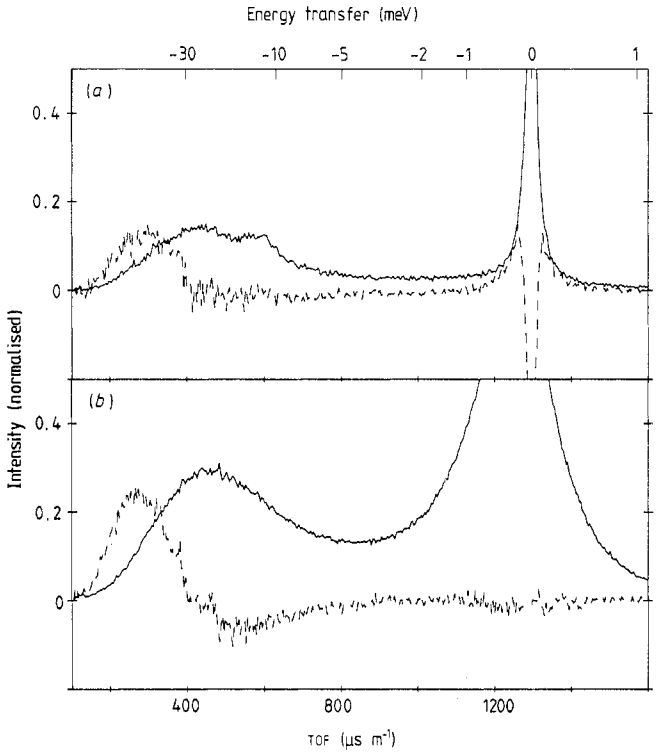

Figure 7. Corrected and normalised intensities $\hat{I}_{\bar{m}\bar{m}}$ (———) and $\hat{I}_{\bar{q}\bar{q}}$ (— — —) for molten LiCl at scattering angles of (*a*) 21.3° and (*b*) 106.4°.

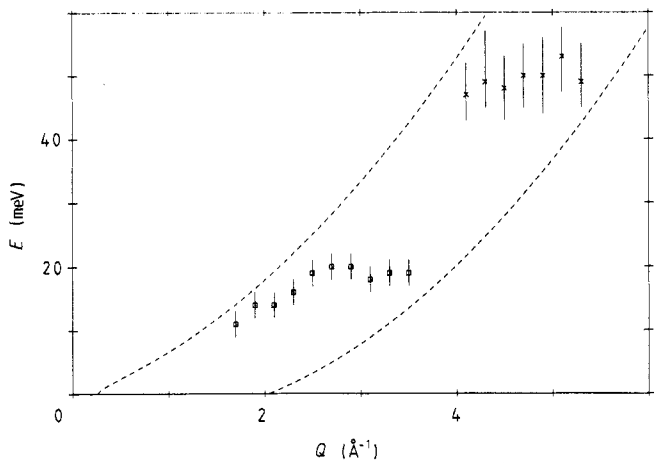

Figure 8. Quasi-dispersion curves derived from peak positions of $\hat{C}^{L}_{\bar{m}\bar{m}}(Q, \omega)$ (⊡) and $\hat{C}^{L}_{\bar{q}\bar{q}}(Q, \omega)$ (×) at constant Q for molten LiCl. The broken curves indicate the experimental (Q, ω) range.

6. Discussion

We have shown that appropriate dynamical variables for molten LiCl in the range $2\ \text{Å}^{-1} < Q < 5\ \text{Å}^{-1}$ are $\bar{m}$ and $\bar{q}$. For CsCl (McGreevy *et al* 1985), m and q are appropriate; the corresponding branches in the quasi-dispersion curve are well separated. In

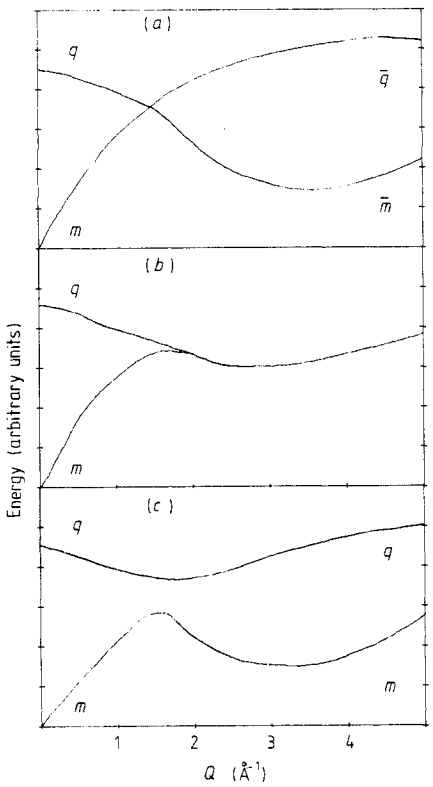

Figure 9. Schematic quasi-dispersion curves for molten alkali chlorides with (*a*) $m_+ < m_-$, (*b*) $m_+ = m_-$ and (*c*) $m_+ > m_-$. Appropriate dynamical variables are indicated.

the case of RbCl (McGreevy and Mitchell 1982), m and q are still good variables but the coupling is stronger and the branches are closer. On the basis of these results, it can be suggested that the crossover from m and q to $\bar{m}$ and $\bar{q}$ will occur when $m_+ = m_-$, i.e. for KCl. The cases $m_+ > m_-$ and $m_+ < m_-$ are inequivalent since the cations and anions are not identical in all respects other than mass and charge; for instance the anion radii and polarisabilities are always larger. In the limit $Q \to 0$, m and q are the correct independent variables for all the salts. We therefore suggest that the quasi-dispersion curves may have the forms shown schematically in figure 9. At $Q = 0$, the variables are m (acoustic mode) and q (optic mode). As Q increases, the energy of the m mode increases (initially with the velocity of sound) and that of the q mode decreases, as for the optic mode in the crystalline state. In the region $1\ \text{Å}^{-1} < Q < 2\ \text{Å}^{-1}$, equivalent to the first Brillouin zone edge in the crystal, the branches approach each other and the modes will couple strongly; at this point, $S_{mq}(Q)$ is a maximum. If $m_+ > m_-$ the branches separate again and variables remain m and q, giving a dispersion as observed in CsCl and RbCl. If $m_+ < m_-$, however, the branches cross and the variables change to $\bar{m}$ and $\bar{q}$, giving a dispersion as observed in LiCl. When $m_+ = m_-$, the variables $\bar{m}$ and q are equivalent, as are $\bar{q}$ and m; the modes remain strongly coupled. For this case the single-particle response frequencies in the high-Q limit are degenerate, also giving a single branch.

While it is not possible to show unequivocally that the spectra for KCl are in agreement with this prediction, the large contribution to $S_T(Q)$ from $S_T(Q, \omega)$ in the high-ω region at $Q \simeq 2\ \text{Å}^{-1}$ is consistent with there being significant mode coupling. Also, if m and q were good variables, then, from the coefficients in table 1, we would expect m to

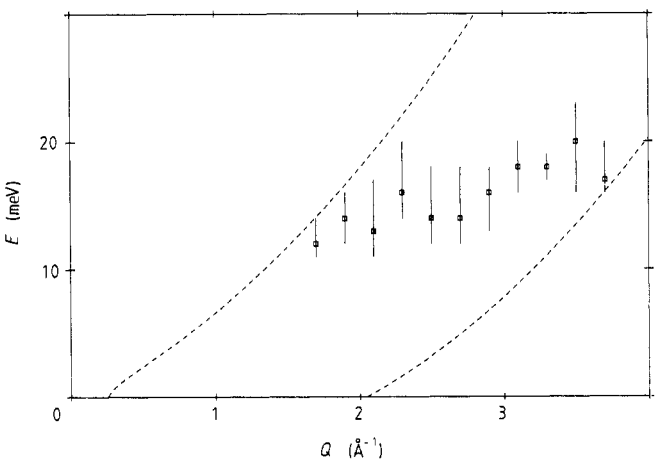

Figure 10. The quasi-dispersion curve derived from peak positions of $C_T^L(Q, \omega)$ at constant Q for molten KCl. The broken curves indicate the experimental (Q, ω) range.

dominate and $C_T^L(Q, \omega)$ should peak at a lower energy (about 10 meV) than is observed (figure 10), while, if $\bar{m}$ and $\bar{q}$ were good variables, $\bar{q}$ would dominate and it should peak at higher energy (about 20 meV). This may be tested by experiments on KCl using isotopic substitution.

The significance of the $m_+ = m_-$ case can be found in the crystalline state as well. The LA and TO modes have a crossover at a Q smaller than the 100 zone edge in NaCl and KCl, while in RbCl and CsCl (although this has a different structure) there is no crossover (Hardy and Karo 1979). It is apparent that the features of the inter-ionic potential which cause these properties in the solid state have a similar effect in the liquid, despite the lack of symmetry in the local structure. It is not yet clear what role the structural coordination, i.e. tetrahedral or octahedral, has in determining the dynamical modes, since it is in itself determined by the inter-ionic potential.

It is not clear what physical significance, if any, may be attributed to the change in dynamical variables from m and q to $\bar{m}$ and $\bar{q}$, although it may of course be alternatively interpreted as a π-phase shift. The change occurs at a Q-value which would lie within the second Brillouin zone in the corresponding crystal; so the process giving rise to this momentum transfer may consist of a combination of elastic and inelastic scattering (equivalent to umklapp scattering), in which case the inelastic part may be either longitudinal or transverse. It will therefore be difficult to attribute scattering in this region to any particular atomic motions without a thorough theoretical treatment of the problem. A series of molecular dynamics simulations of ionic melts with different masses may be used to test the proposals regarding the form of the dispersion curves, although again it will be difficult to determine which atomic motions correspond to which dynamical variables.

7. Conclusions

A qualitative description of the collective dynamics in molten alkali chlorides, in the momentum transfer range corresponding to motions in the first coordination shell, can now be made in terms of the appropriate dynamical variables. There are both in-phase and out-of-phase motions of anions and cations, although which is of higher energy depends on the mass ratio. It seems likely that the same pattern will be followed for the

other alkali halides, although this will be hard to test owing to the lack of suitable isotopes. A more detailed description of the alkali chlorides is also not feasible, since the small differences between Cl isotope scattering lengths make the experimental accuracy required too great. Only in the unique case of NiI_2 (Wood 1988) is it possible to separate quantitatively all the partial dynamical structure factors. Further insight may be given by molecular dynamics simulations, but these will require a better treatment of ionic polarisability (Dixon 1983, McGreevy *et al* 1984) since dynamics are far more sensitive to such aspects of the inter-ionic potential than structure.

Acknowledgments

We wish to thank The Royal Society (RLM), the Sörös Foundation (LP) and the Science and Engineering Research Council for support for this work. We also thank the staff of the Institut Laue–Langevin, particularly Dr R White, for assistance with experiments. Special thanks are due to Dr R Ward of the Clarendon Laboratory Crystal Growth Group for careful preparation of the anhydrous samples. The authors are grateful to one of the referees for pointing out some numerical errors in the original text.

References

Dixon M 1983 *Phil. Mag.* B **48** 13
de Gennes P G 1959 *Physica* **25** 825
Hardy J R and Karo A M 1979 *The Lattice Dynamics and Statics of Alkali Halide Crystals* (New York: Plenum)
Howe M A and McGreevey R L 1988 *Phil. Mag.* B **58** 485
Locke J, McGreevy R L, Messoloras S, Mitchell E W J and Stewart R J 1985 *Phil. Mag.* B **51** 301
Margaca F M A, McGreevy R L and Mitchell E W J 1984 *J. Phys. C: Solid State Phys.* **17** 4725
McGreevy R L 1987 *Solid State Phys.* **40** 247 (New York: Academic)
McGreevy R L and Mitchell E W J 1982 *J. Phys. C: Solid State Phys.* **15** L1001
—— 1985 *J. Phys. C: Solid State Phys.* **18** 1163
McGreevy R L, Mitchell E W J and Margaca F M A 1984 *J. Phys. C: Solid State Phys.* **17** 775
McGreevy R L, Mitchell E W J, Margaca F M A and Howe M A 1985 *J. Phys. C: Solid State Phys.* **18** 5235
Wood N D 1988 private communication